Geomechanics and Engineering, *Vol. 30, No. 5 (2022) 423-435*
https://doi.org/10.12989/gae.2022.30.5.423

Evaluation of blasting vibration with center-cut methods for tunnel excavation

Seung-Joong Lee[1a], Byung-Ryeol Kim[2b], Sung-Oong Choi*[3] and Nam-Soo Kim[4c]

[1]*Smart Mining Team, Hanwha Corporation/Global, Pangyo-ro 305, Bundang-gu, Seongnam-si, Gyeonggi-do, Korea*
[2]*Energy Environment Team, Korea Institute of Limestone & Advanced Materials, Udeok-gil 18-1, Maepo-eup, Danyang-gun, Chungcheongbuk-do, Korea*
[3]*Department of Energy and Resources Engineering, Kangwon National University, Gangwondaehakgil 1, Chuncheon-si, Gangwon-do, Korea*
[4]*NSB Now ENC, Ttukseom-ro 19, Gwangjin-gu, Seoul-si, Korea*

(*Received December 31, 2021, Revised August 1, 2022, Accepted August 12, 2022*)

Abstract. Ground vibration generated repeatedly in blasting tunnel excavation sites is known to be one of the major hazards induced by blasting operations. Various studies have been conducted to minimize these hazards, both theoretical and empirical methods using electronic detonator, the deck charge method, the center-cut method among others Among these various existing methods for controlling the ground vibration, in this study, we investigated the cut method. In particular, we analyzed and compared the V-cut method, which is commonly used in tunnel blasting, to the double-drilled parallel method, which has recently been introduced in tunnel excavation site. To understand the rock fragmentation efficiency as well as the ground vibration controllability of the two methods, we performed in-situ field blasting tests with both cut methods at a tunnel excavation site. Additionally, numerical analysis by FLAC3D has been executed for a better understanding of fracture propagation pattern and ground vibration generation by each cut method. Ground vibration levels, by PPVs measured in field blasting tests and PPVs estimated in numerical simulations, showed a lower value in the double-drilled parallel compared with the V-cut method, although the exact values are quite different in field measurement and numerical estimation.

Keywords: blasting vibration; cut method; double-drilled parallel cut; finite difference method; V-cut

1. Introduction

Blasting vibration must be kept within the limits of the standards because repeated ground vibrations induced by blasting operations in tunnel excavation sites can cause severe environmental concerns (Korea Environment Institute 2015). To resolve this, numerous blasting methods have been proposed to control the blasting vibrations and their field applicability explored (Oh *et al*. 2017, Song *et al*. 2017, Lee *et al*. 2018, Ozacar 2018, Uyar *et al*. 2019, Dimitraki *et al*. 2021).

Since field accessibility poses numerous experimental restrictions, researchers have mainly numerically simulated the distribution pattern of the blast-damaged zone (BDZ), fracture propagation, and vibration-reduction effect. For example, Park *et al*. (2009) quantitatively analyzed the ground vibration-reduction effect of the line-drilling method by PFC2D and AUTODYN3D. Lu *et al*. (2011) compared the results of their numerical simulations of blasting vibration to the vibration values measured at a tunnel excavation site. Furthermore, to understand the effect of a blasting pressure on the surrounding rock masses, Yilmaz and Unlu (2013) conducted FLAC3D simulations using various types of rocks, the detonating pressure, and in-situ stresses as input data. They concluded that the range of the tensile failure zone increases as the detonating pressure and horizontal principal stresses increase. Qiu *et al*. (2018) indicated that the overlap of the stress waves is highest during the same detonation delay.

This study focuses on the double-drilled parallel cut method, which was introduced to reduce the blasting vibrations in 2007 (Won and Lee 2007). Various studies have done test blasting at sites to verify the vibration reduction effect of the double-drilled parallel cut method (Kim 2016, Lee and Kim 2016). However, the fracture mechanism of the method has not been investigated due to the risk involved in the field blasting work. Therefore, in this study, we analyzed the fracture mechanism and the vibration reduction effect through a three-dimensional numerical analysis and examine the applicability of the numerical model.

For this purpose, two blasting operations were performed at a test site using the V-cut method and double-drilled parallel cut method design. The ground vibrations from blasting operations were monitored for each blasting test. Furthermore, to analyze the fracture mechanism and overcome the restrictions in terms of the required number and costs of field blasting tests, the FLAC3D finite-difference code was applied to numerically simulate the

*Corresponding author, Professor
E-mail: choiso@kangwon.ac.kr
[a]Ph.D.
E-mail: sjlee3601@hanwha.com
[b]Ph.D.
E-mail: parallel@kilam.re.kr
[c]Ph.D.
E-mail: nsbpro@hanmail.net

ISSN: 2005-307X (Print), 2092-6219 (Online)

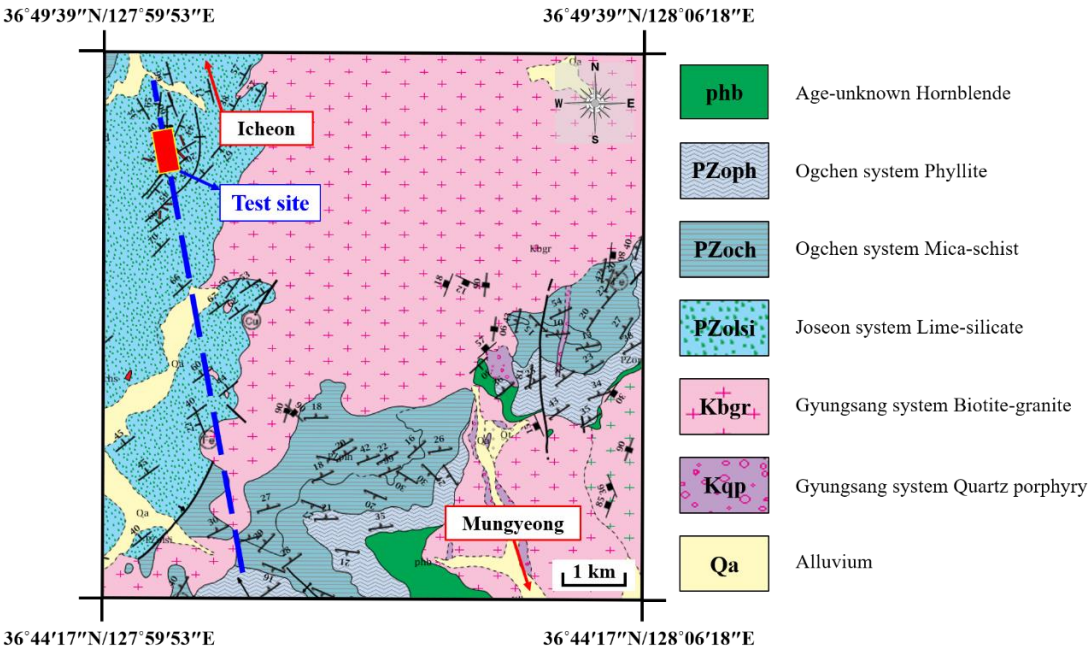

Fig. 1 Geological features of the test site (The bold dotted line denotes a proposed railway route)

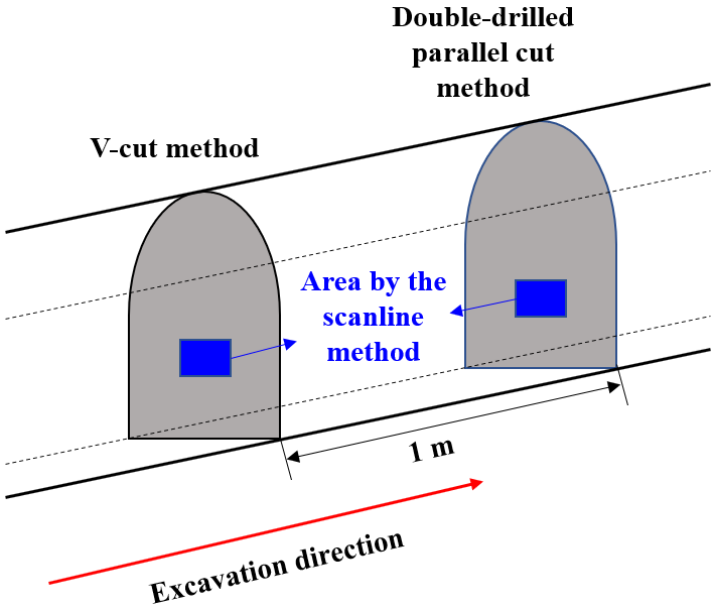

Fig. 2 Each area by the scanline method in the tunnel excavation site

blasting process. Then, the blasting vibrations obtained in the numerical simulation model were compared to the real blasting vibration values observed in the field test to evaluate the applicability of numerical simulations for blasting vibration analysis.

2. Field blasting operations

2.1 Geology of the test site

Fig. 1 shows the geological features of the test site area. The geology of this area mainly consists of age-unknown Ogcheon Supergroup (OSG), early Paleozoic Joseon Supergroup (JSG), early Mesozoic Daedong Supergroup (DSG), and igneous rocks invading the Mesozoic layer above a Precambrian gneiss complex (KIGAM 2021). Fig. 2 shows a schematic diagram of the field survey to rate the rock masses in the tunnel excavation site. The Scanline method is a common way to survey discontinuity distribution. It sets up a scanline with a specific length of exposed rock and estimates dip direction and dip, roughness, and spacing of discontinuity intersecting with the scanline. Based on the scanline method, we evaluated the rock discontinuity distribution pattern around the tunnel face. The rock mass rating was conducted after considering the results of the laboratory and borehole inspection tests. Fig. 3 and Table 1 show the results of the rock joint

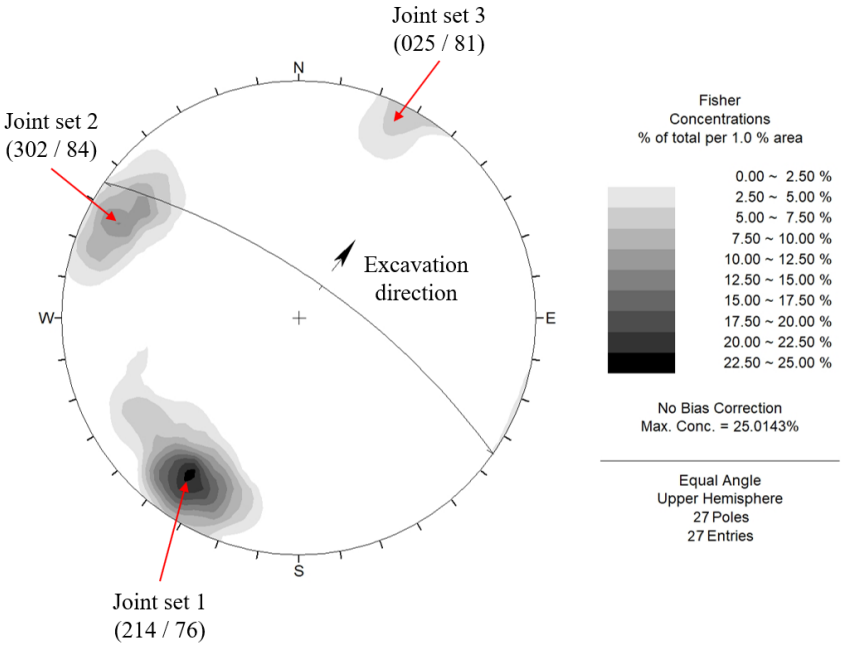

Fig. 3 Joint distribution pattern in the tunnel excavation site

Table 1 Results of the joint distribution pattern in the tunnel excavation site

Face number	Joint set 1	Joint set 2	Joint set 3
	Dip direction/ Dip (°)	Dip direction/ Dip (°)	Dip direction/ Dip (°)
1	209/70	298/82	-
2	218/82	305/86	025/81
Average	214/76	302/84	025/81

distribution analysis. There were three major joint sets in the test area, and the main set exhibited a dip direction of 214° and a dip angle of 77°, which are almost perpendicular to those of the other joint sets. Table 2 shows the rock mass rating results at the test site.

2.2 Center-cut methods

In tunnel blasting, the center-cut method is classified into a parallel cut method and an inclined cut method depending on the method for forming the first free face. First, we applied the v-cut method and double-drilled parallel cut method, which correspond to an inclined cut method and a parallel cut method, respectively.

2.2.1 V-cut method

In the v-cut method, holes are drilled symmetrically to each other in an inclination angle of 60° to 70° with respect to the tunnel face. The holes were spaced at an interval of 20 cm with respect to their bottoms. The charge operation was performed as concentric charge to form a high density at the bottom so that a free face can be generated more easily. The method requires a relatively small number of drilled holes per unit area, however, it is limited by the section width of the tunnel because inclined drilling operations should be performed in bilateral symmetry. In addition, the method does not allow for deep drilling. Therefore, the method has a shorter excavation length per

Table 2 Rock mass rating results for the tunnel excavation site

Face number			1		2		Average rating
			Value	Rating	Value	Rating	
Parameter	Intact rock strength		50~100 MPa (92 MPa)	7.0	50~100 MPa (98 MPa)	7.0	7.0
	RQD		50~75% (71.2%)	13.0	50~75% (60.4%)	13.0	13.5
	Spacing of joint set 1		0.6~2.0 m (0.8 m)	15.0	200~600 mm (55 mm)	10.0	12.5
	Condition of joint set 1	Persistence	10~20 m	1.0	10~20 m	1.0	1.0
		Aperture	0.1~1.0 mm	4.0	0.0	6.0	5.0
		Roughness	Slightly rough	3.0	Rough	5.0	4.0
		Infilling	Hard filling<5 mm	2.0	Hard filling<5 mm	2.0	2.0
		Weathering	Slightly	5.0	Slightly	5.0	5.0
		Subtotal	-	15.0	-	19.0	17.0
	Ground water condition		Wet	7.0	Damp	10.0	8.5
	Total rating		57.0		59.0		58.0
	Grade		III		III		III

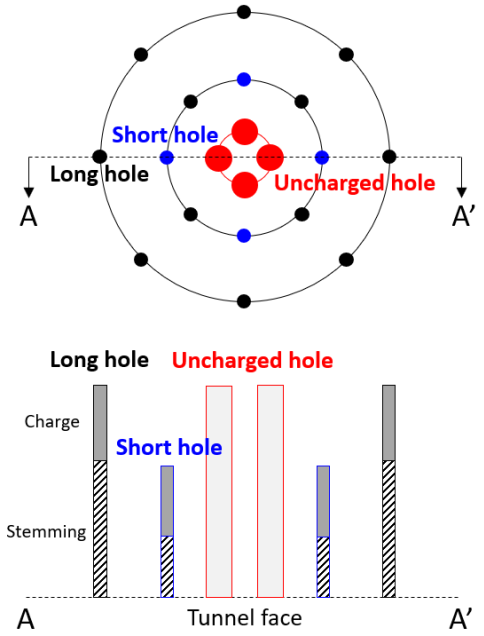

Fig. 4 Schematics of the double-drilled parallel cut method

blasting operation, compared with other center-cut methods. In addition, lateral holes can experience drilling error, and the initial vibration caused by concentric charge cannot be prevented.

2.2.2 Double-drilled parallel cut method

The double-drilled parallel cut method is a method developed by improving the drilling pattern of the cylinder-cut method, which is one of the parallel cut methods. Double-drilled parallel cut method was developed to improve the center-cut part blasting efficiency in tunnels and reduce noise and vibration. Based on the conventional parallel method, the long holes and short holes are alternately drilled with uncharged holes at the center in order to minimize the distance between a charged hole and an uncharged hole. This method makes it easier to extract the rocks blasted in the direction of a free face, and allows for the center-cut blasting with a small charge weight per hole to suppress the vibration in the initial stage of the blasting.

Fig. 4 shows a plan and cross-sectional view of the double-drilled cut method, and Fig. 5 shows the individual steps of the blasting mechanism of the double-drilled parallel cut method. In the 1st step, short holes having a short burden to an uncharged hole are detonated (Fig. 5(a)). The initial vibration can be controlled through the free face effect of the uncharged hole. In 2nd step, the first free face is expanded by short hole blasting (Fig. 5(b)). In the 3rd step, long holes are detonated (Fig. 5(c)). Since the expansion of the first free face in the 2nd step has weakened the confinement force of rock mass, the secondary vibration can be controlled. In the 4th step, the second free face is expanded to the designed excavation length (Fig. 5(d)). Therefore, the double-drilled parallel cut method can effectively control the vibration, because the short holes and long holes are sequentially denoted with uncharged holes at the center, making it easier to form and extend free faces while reducing the confinement force of rock mass in stages.

2.3 Field test blasting

Blasting operations were conducted at the test site by both the V-cut method and the double-drilled parallel cut

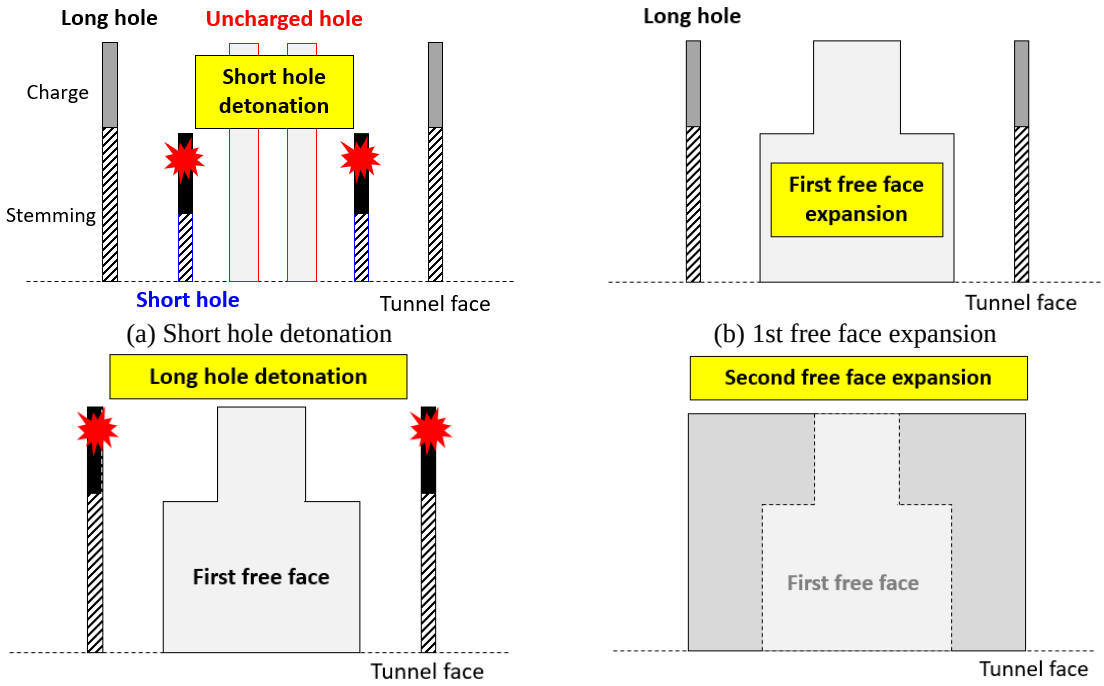

(a) Short hole detonation

(b) 1st free face expansion

(c) Long hole detonation

(d) 2nd free face expansion

Fig. 5 Blasting mechanism of double drilled parallel cut method

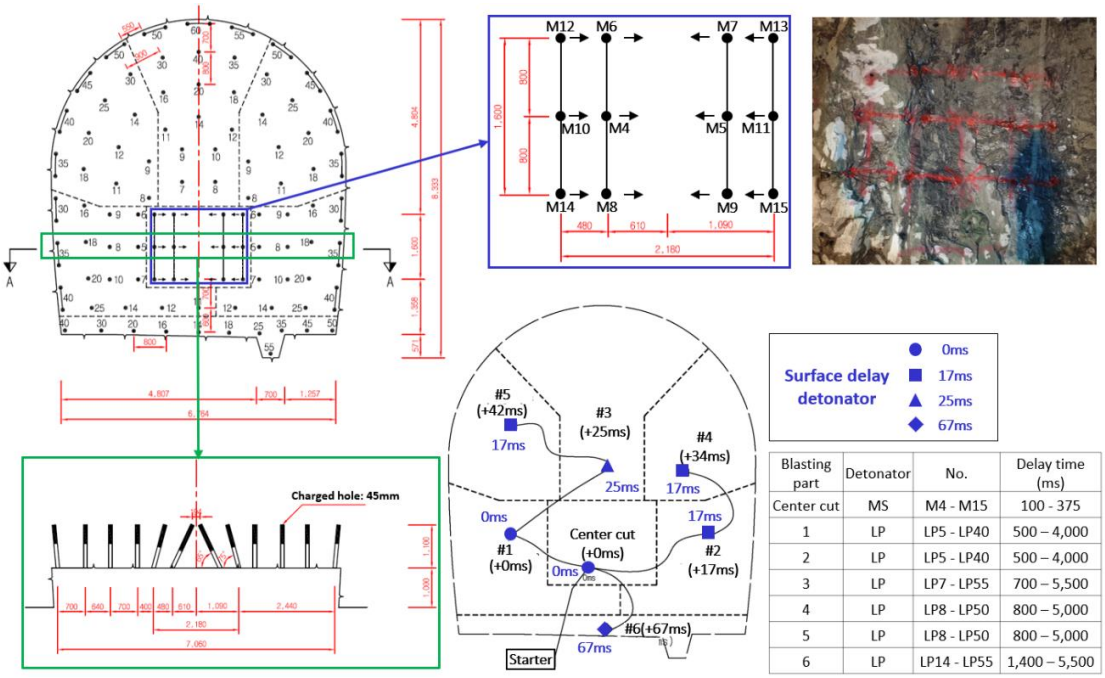

Blasting part	Detonator	No.	Delay time (ms)
Center cut	MS	M4 - M15	100 - 375
1	LP	LP5 - LP40	500 – 4,000
2	LP	LP5 - LP40	500 – 4,000
3	LP	LP7 - LP55	700 – 5,500
4	LP	LP8 - LP50	800 – 5,000
5	LP	LP8 - LP50	800 – 5,000
6	LP	LP14 - LP55	1,400 – 5,500

(a) V-cut method

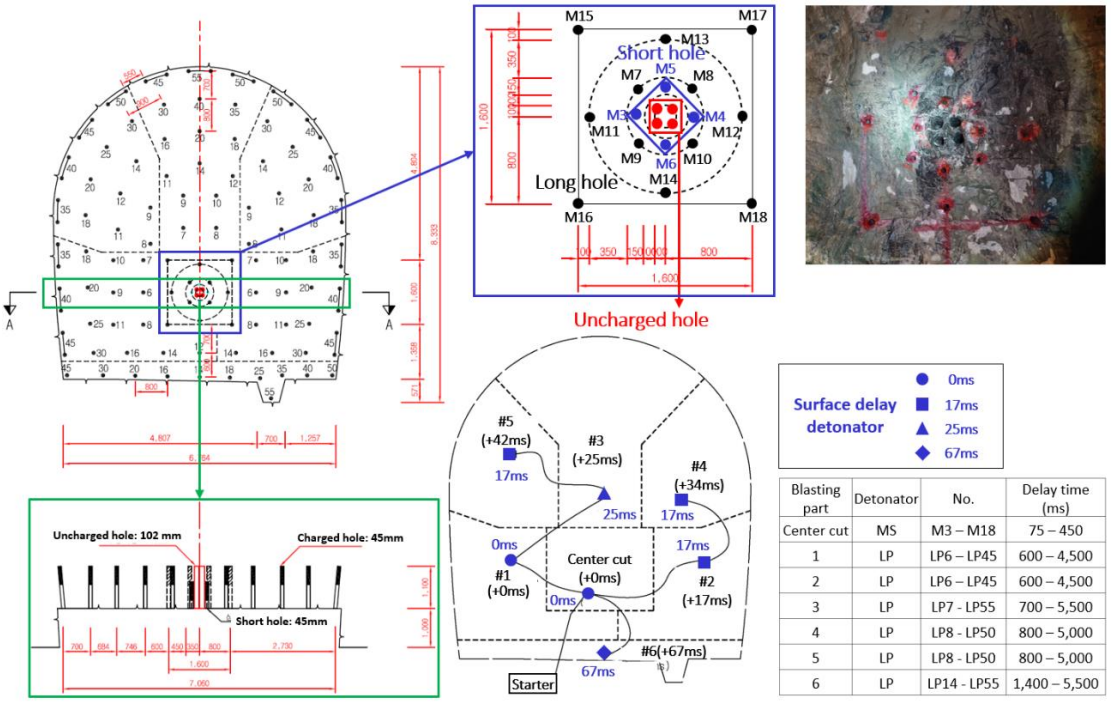

Blasting part	Detonator	No.	Delay time (ms)
Center cut	MS	M3 – M18	75 – 450
1	LP	LP6 – LP45	600 – 4,500
2	LP	LP6 – LP45	600 – 4,500
3	LP	LP7 - LP55	700 – 5,500
4	LP	LP8 - LP50	800 – 5,000
5	LP	LP8 - LP50	800 – 5,000
6	LP	LP14 - LP55	1,400 – 5,500

(b) Double-drilled parallel cut method

Fig. 6 Schematics of the cut method in tunnel blasting

method. The V-cut method is commonly used in underground blasting operations, and generally uses the two 60° inclined holes on either side of the central axis (Fig. 6(a)). On the other hand, the double-drilled parallel cut method uses an uncharged central hole surrounded by long/short charged holes (Fig. 6(b)). These long and short holes are cross-drilled and detonated with delayed timing to eliminate the dead pressure and the induced explosion.

Table 3 summarizes the blasting patterns applied to each cut method. Emulsion explosives are used in test blasting, and the diameter of each charging hole is 45 mm (Table 4). A non-electric detonator was used for blast hole detonation. For a part of the central cut, MS (Milli Second) detonator with 25 ms delay time was used. For the rest, LP (Long Period) detonator was used.

To measure the blasting vibration caused by each cut method, two blasting vibration measurement devices were installed approximately 59 m (measurement A) and

Table 3 The blasting patterns in each cut method

Method		V-cut method	Double-drilled parallel cut method
Excavation length (m)		1.0	1.0
Drilling length (m)		1.2	1.1 (Long hole)/0.7 (Short hole)
Charged hole	Diameter of hole (mm)	45	45
	The number of holes (ea)	113	117
Uncharged hole	Diameter of hole (mm)	-	102
	The number of holes (ea)	-	4
Cut pattern charge (kg)		7.2	8.0
Total charge (kg)		53.8	54.6
Specific charge (kg/m^3)		1.066	1.082
Cross section area (m^2)		50.462	50.462

Table 4 Property of explosives

Explosives	Blasting part	Ave. Detonation velocity (m/sec)	Bulk density (g/cc)	Heat energy (kcal/kg)	Gas volume (l/kg)	Water-proofing
Emulsion explosives	Central, Expanded, Bottom	6,000	1.22 ~ 1.26	1,398	675	Excellent
Emulsion explosives for control blasting	Outline	4,000	1.0	735	870	Excellent

approximately 77 m (measurement B) away from the excavation section (Fig. 7). Table 5 shows the specifications

Table 5 Specifications of SV1

Maximum vibration measurement range	100 mm/sec
Vibration frequency range	1-80 Hz
Vibration precision	1%
Vibration resolution	0.01 mm/sec
Noise measurement range	30-130 dBA
Noise frequency range	20 Hz-8 kHz
Noise precision	ICE 60651:1979 Type 2
Noise data	L_{max}, L_{eq}
Measuring sample rate	1,024 samples/sec
Storage sample rate	1,024 samples/sec

of the SV-1 blasting vibration measurement tool from the SV Corporation, and Fig. 8 shows the measured vibration waveform of the V-cut method and double-drilled parallel cut method at measurement A.

Table 6 summarize the peak particle velocity (PPV) pattern measured for each cut method blasting. As shown in this table, the PPV generated by the V-cut method is slightly higher than that generated by the double-drilled parallel cut method. Specifically, the PPV generated by the double-drilled parallel cut method, was 15.46% lower at measurement A and 46.25% lower at measurement B than that generated by the V-cut method at each measurement.

3. Numerical simulation

3.1 Numerical model and conditions

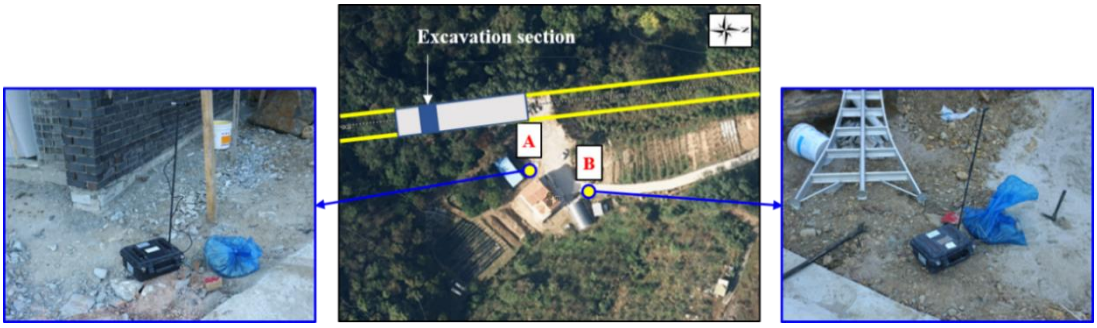

Fig. 7 Blasting vibration field measurement

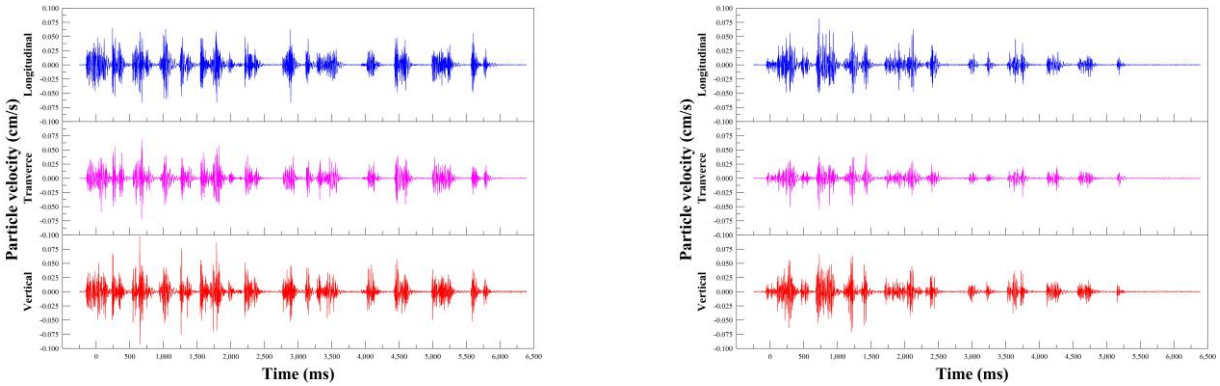

(a) V-cut method (b) Double-drilled parallel cut method

Fig. 8 Velocity versus time graph at a distance of 59.1 m from the tunnel face (measurement A)

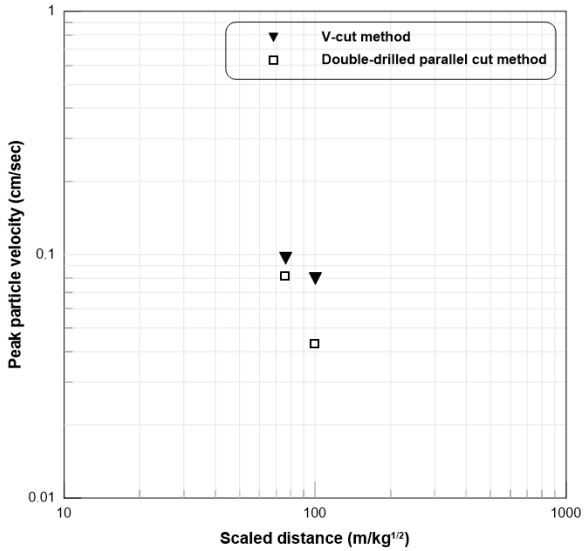

Fig. 9 The relation between PPV and the scaled distance in each cut method

We used FLAC3D, a finite-difference code developed by Itasca, to simulate the field blasting operation and compare the field vibration results. To ensure efficient numerical analysis, a part of a central cut was modeled. Numerical models for both the V-cut and double-drilled parallel cut were generated by the Griddle program from Itasca, as shown in Fig. 10, with dimensions of 14×2×14 m. The location of the center-cut was approximately 50 m away from the ground. The center-cut part was generated in the center of the numerical model. A uniform pressure of 1,138 kPa (rock weight, $r = 2{,}700\ \mathrm{kg/m^3}$) was applied to the top of the model, stimulating ground stress at a depth of 43 m. Furthermore, to minimize the reflection effect of vibration waves that may be generated at the boundary of the numerical model, we applied an infinite boundary condition for all boundaries. The blasting pressure from the hole was also designed to apply radially in the numerical model, and the delay duration was designed based on the blasting pressure pattern.

The input data for the numerical analysis were obtained from static and dynamic laboratory tests conducted on rock samples collected from the field site (Table 7). The static tests conducted on the rock samples were uniaxial compressive test, triaxial compressive test, Brazilian test and density measurement test based on the standard method as set by KSRM (Korea Society for Rock Mechanics). The dynamic test was the free-free resonant column test in accordance with ASTM C 215. This test applies the impact echo method, i.e., it applies an impact in the longitudinal direction of the specimen using an impact hammer, as shown in Fig. 11, while the resonance frequency is analysed by measuring the generated vibration. Then, the dynamic Young's modulus and damping ratio are calculated using this resonant frequency. The results of the free-free resonant column test indicate that the damping ratios of the longitudinal and torsional modes are 1.27% and 1.58%, respectively.

The blasting pressure is vital as a boundary condition when simulating blasting properties in a numerical model. Various equations have been proposed in both theoretical and empirical studies, and most of these equations were established with the density of explosives and detonating velocity as parameters. In this study, the blasting pressure was estimated from the equation developed by the National Highway Institute (1991) (Eq. (1)).

$$P_d = \frac{449.93}{1+0.8SG_e} SG_e D_e^2 \quad (1)$$

where P_d is the maximum blasting pressure (Pa), SG_e is the explosives density (g/cm^3), and D_e is the explosives detonating velocity (m/sec).

However, the real dynamic pressure acting on the wall of the blasting hole varies with time; thus, the time-history blasting pressure should be factored in the numerical analysis for more realistic simulations. The window function suggested by Starfield and Pugliese (1968) is typically used in the damping equation (Eqs. (2)-(3)).

$$P_d(t) = 4P_B \left\{ \exp\left(\frac{-Bt}{\sqrt{2}}\right) - \exp\left(-\sqrt{2}Bt\right) \right\} \quad (2)$$

$$P_B = P_d \left(\frac{d_c}{d_h}\right)^3 \quad (3)$$

where $P_d(t)$ is the maximum blasting pressure according to time-history (Pa), P_B is the pressure acting on the wall of hole (Pa), B is a constant for the blasting pressure (=16,338), P_d is the maximum blasting pressure (Pa), d_c is the diameter of the explosives (mm), and d_h is the diameter of the blasting hole (mm).

3.2 Numerical results

3.2.1 Blasting pressure propagation

In our numerical analysis, the simulated sequence of the explosion of each detonator was the same as that of the field blasting operations. Furthermore, the time steps for numerical analysis were applied until the blasting pressure propagated up to the model boundary. Fig. 12 shows the numerical results of the principal stress distribution around the central cut hole. As shown in figures (a) and (b), the

Table 6 Results of the field blasting operations

Method	Measurement	Distance (m)	Charge weight per delay (kg/delay)	Velocity (cm/sec)				Scaled distance (m/kg$^{\frac{1}{2}}$)	Reduction ratio compared to V-cut (%)
				Longitudinal	Transverse	Vertical	PPV		
V-cut	A	59.10	0.60	0.067	0.072	0.097	0.097	76.30	-
	B	77.89	0.60	0.058	0.023	0.080	0.080	100.56	-
Double-drilled parallel cut	A	58.58	0.60	0.082	0.054	0.065	0.082	75.63	15.46
	B	77.32	0.60	0.043	0.016	0.038	0.043	99.82	46.25

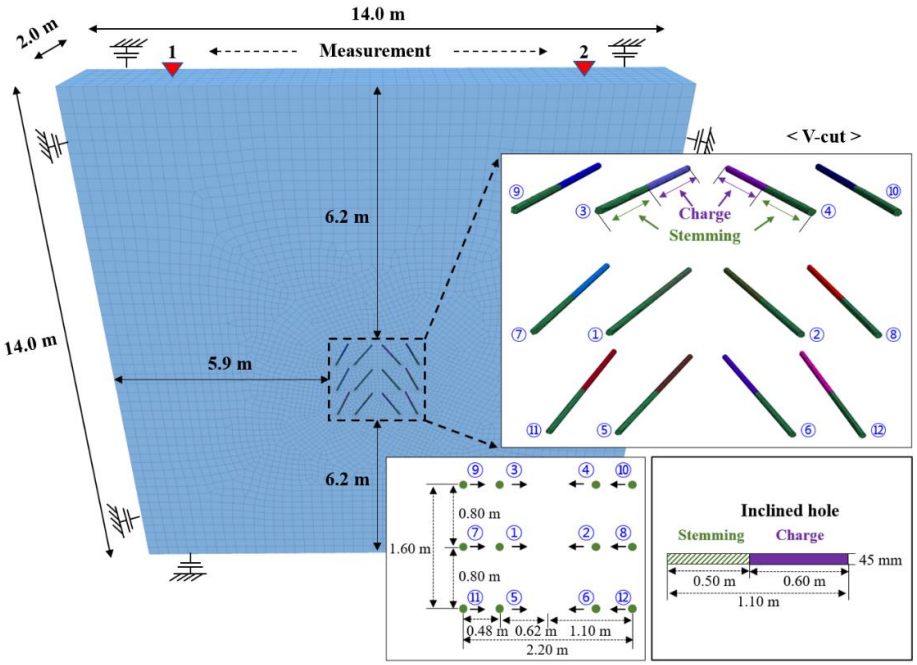

(a) V-cut method

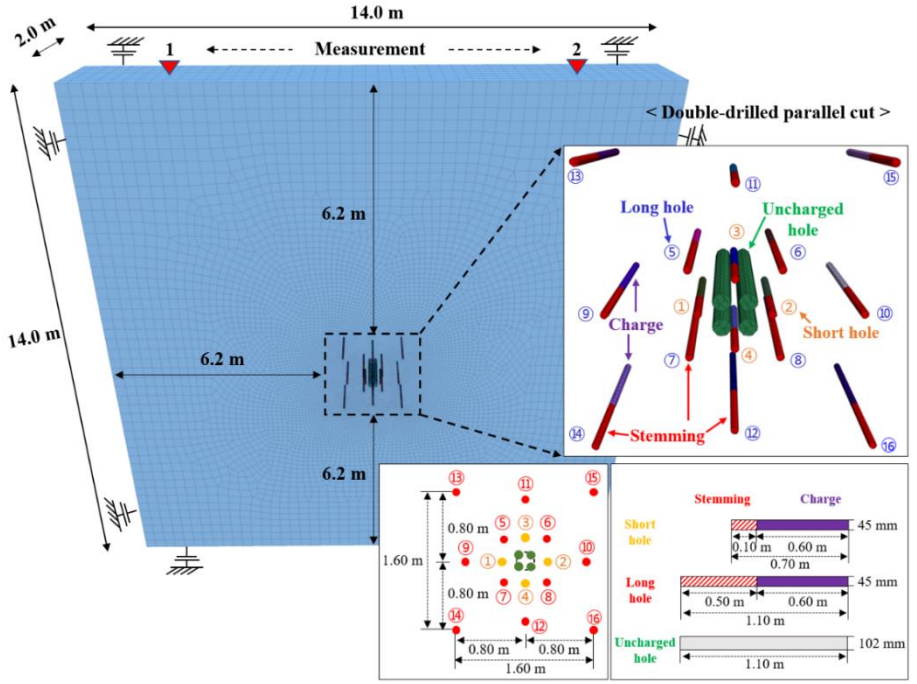

(b) Double-drilled parallel cut method

Fig. 10 Three-dimensional numerical models for each cut method and their boundary conditions

maximum principal stress occurs radially around the first blasting hole for both cut models. The maximum principal stress occurring in rock mass around the blasting hole is 300 MPa in the V-cut model and 80 MPa in the double-drilled parallel cut model.

The maximum principal stress was lower in the double-drilled cut model because the free face effect of the four uncharged holes located at the center of the center-cut part propagated and attenuated the pressure in the direction of the uncharged holes having the weaker confinement force of rock mass. On the contrary, in the V-cut model where there is no uncharged hole and the hole bottom interval was 20 cm, when the blasting holes were sequentially detonated, the pressure in the adjacent blasting spaces was amplified, resulting in a higher maximum principal stress than that of the double-drilled cut model.

We confirmed that the blasting dynamic pressure applied to each model is spread fully around rock mass. Since the fifth blasting hole detonates, however, tension fracture has occurred in the radial direction more extensively in the double-drilled parallel cut model than in the V-cut model.

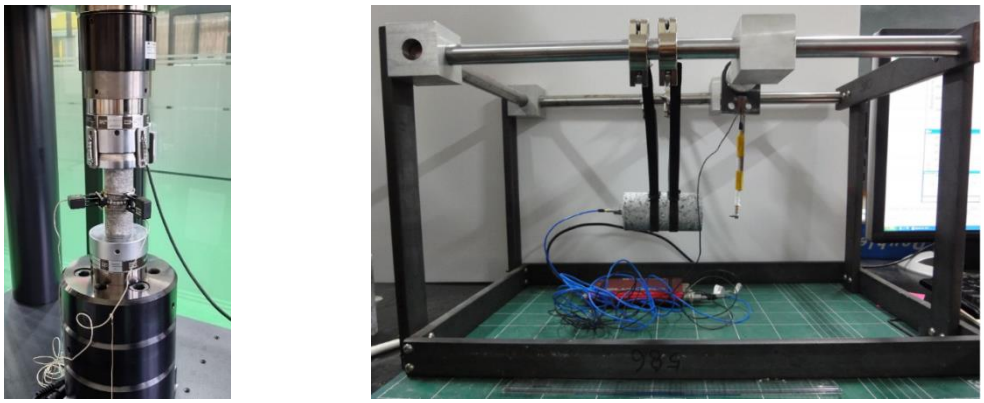

(a) Uniaxial compressive test (b) Free-free resonant column test

Fig. 11 Static and dynamic laboratory tests

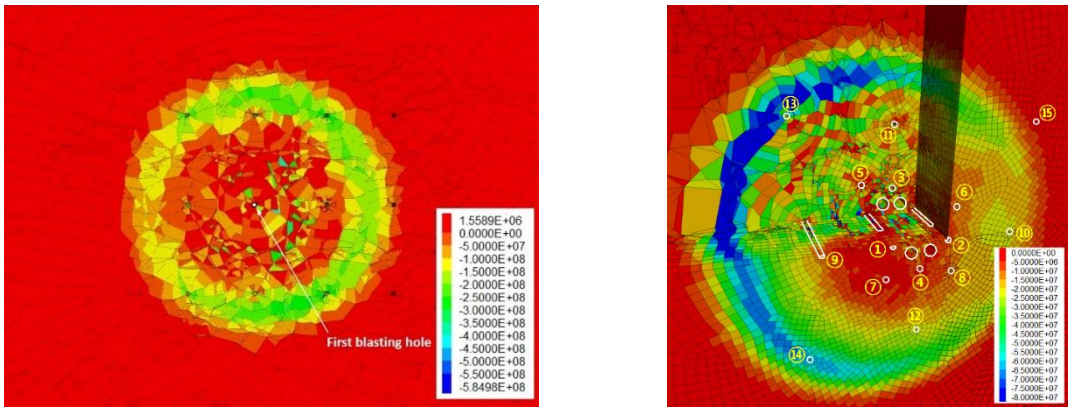

(a) V-cut method (b) Double-drilled parallel cut method

Fig. 12 Principal stress distributions around the central cut after the first hole blasting

Table 7 Input data for numerical analysis

Static laboratory test						
Density (kg/m^3)	Young's modulus (GPa)	Poisson's ratio	Cohesion (MPa)		Friction angle (°)	Tensile strength (MPa)
2,700	25.45	0.22	16.8		44.0	9.8
Dynamic laboratory test						
Mode	Velocity (m/sec)	Resonant frequency (Hz)	0.707		Damping ratio (%)	Dynamic Young's modulus (GPa)
			*f*1 (Hz)	*f*2 (Hz)		
Longitudinal	4.125	15.788	15.588	15.988	1.27	35.52
Torsional	2.253	11.488	11.288	11.650	1.58	12.68

3.2.2 Fracture distribution

Fig. 13 shows the fracture distribution in the double-drilled parallel cut model. In the initial stage of detonation, shear and tension fractures occur, with the latter occurring towards the uncharged hole with high possibility to form a free face. After detonation, the shear and tension fractures gradually expanded.

Fig. 14 shows the cross-sectional view of the fracture of the charge length generated by the detonation of each blasting hole in the V-cut model and double-drilled parallel cut model. The fracture expanded from the center to the edge in the numerical model as each blasting hole detonated sequentially. On comparing two cut models, shear fracture occurs dominantly in the two cut methods when the first blasting hole detonates. Also, the fracture area occurs in a similar way until the second blasting hole detonates. Tension and shear fractures, after the final blasting hole detonates, occur more extensively and gradually in the double-drilled parallel cut model than in the V-cut model. This is because free face expansion occurs significantly due to the uncharged hole located at the center of the double-drilled parallel cut model. Specifically, as shown in Fig. 13, when the short hole detonated, the blasting pressure and fracture propagated in the direction of the uncharged hole having the weaker confinement force of rock mass. This means that the free face expansion in the direction of the uncharged hole was effective. When the long hole detonated, the rock mass destruction occurred effectively up to that the excavation length and fracture caused by short hole blasting. Therefore, in the double-drilled parallel cut method, since the positions of charging at the short hole and long hole are not on the same horizontal line, it was

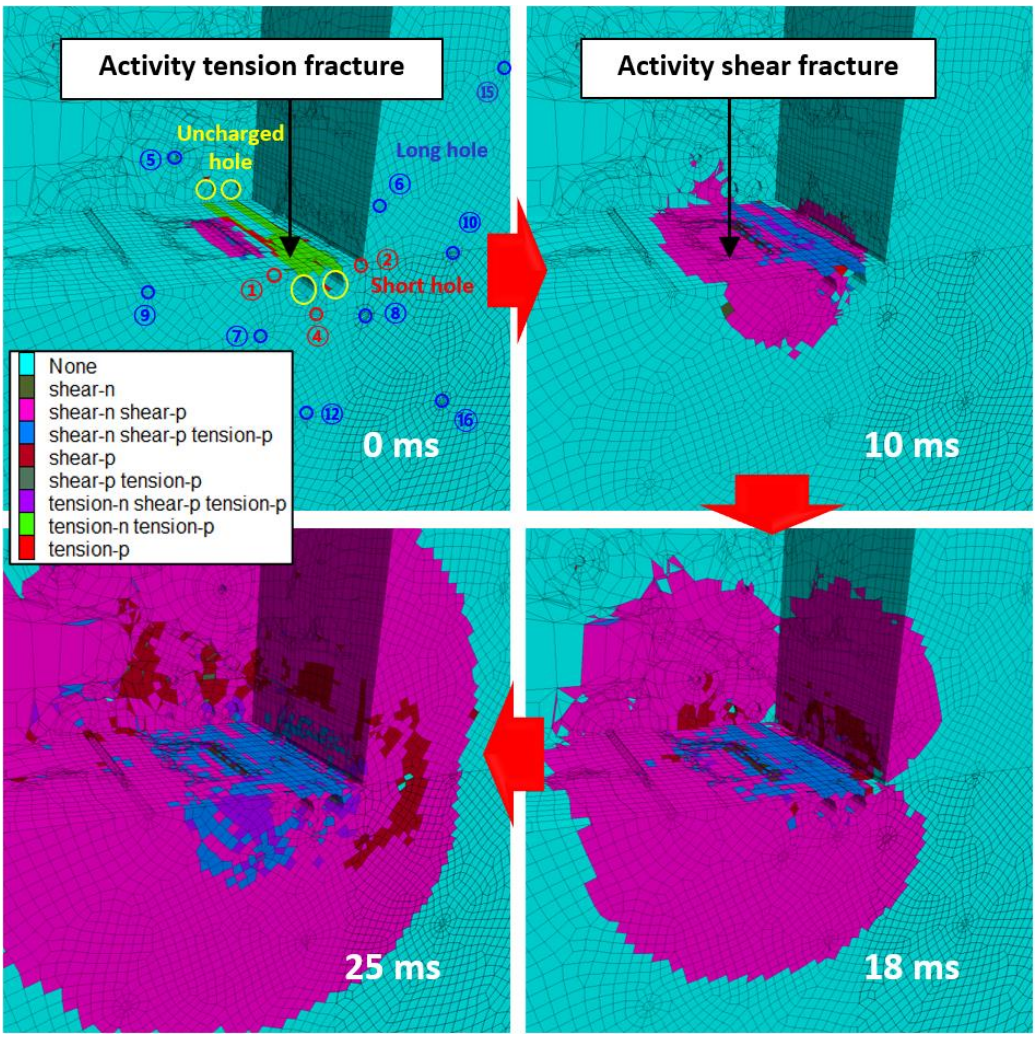

Fig. 13 Fracture distribution for the double-drilled parallel method

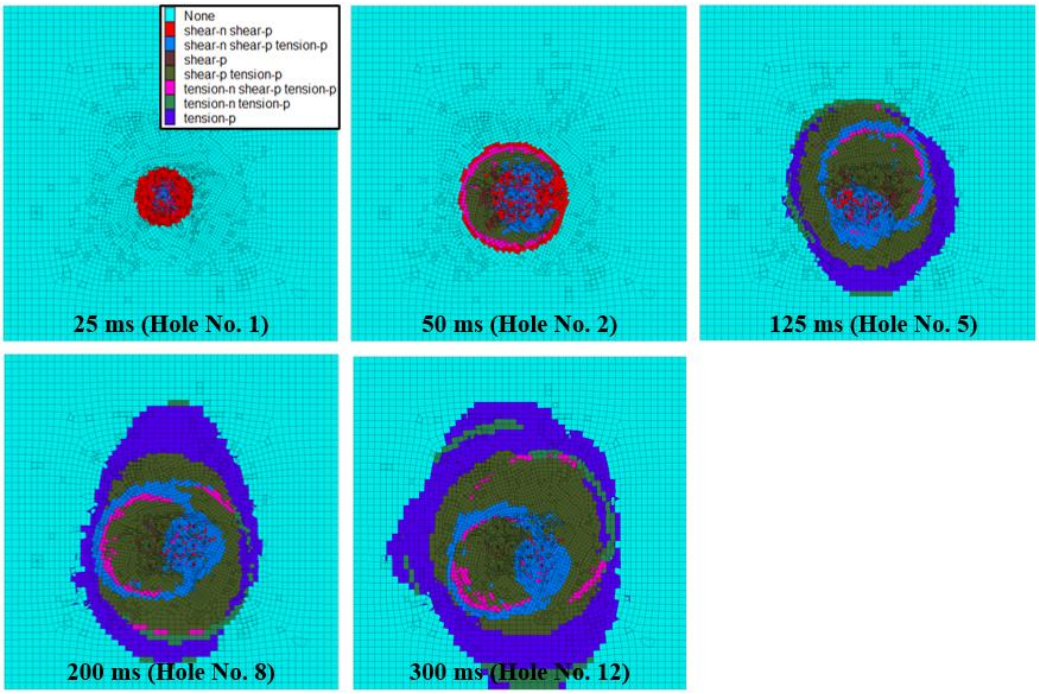

(a) V-cut method

Fig. 14 Fracture propagation aspect by detonation of blasting holes

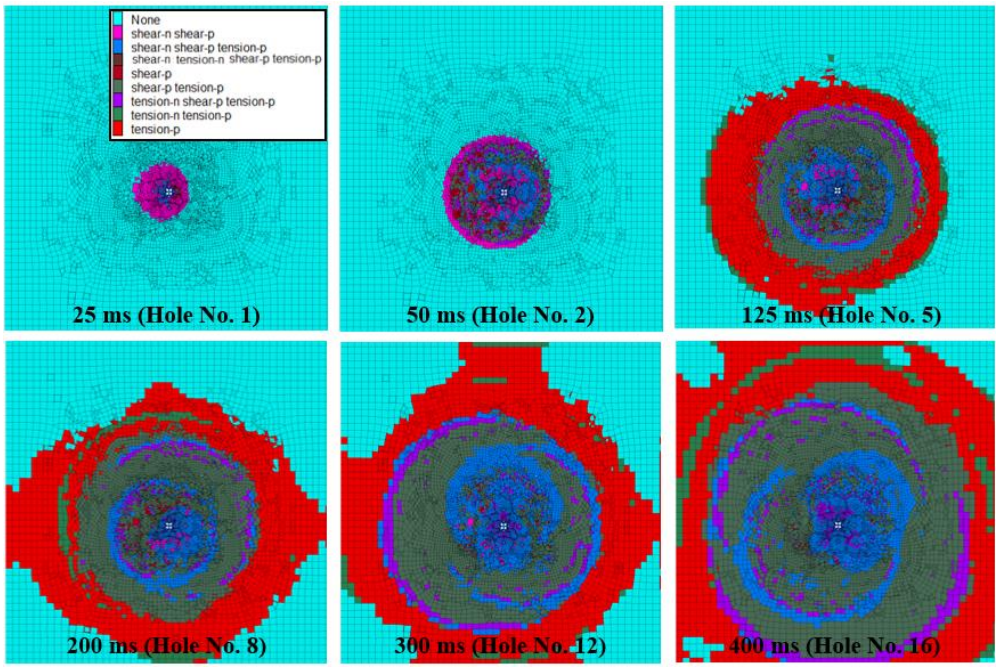

(b) Double-drilled parallel cut method

Fig. 14 Continued

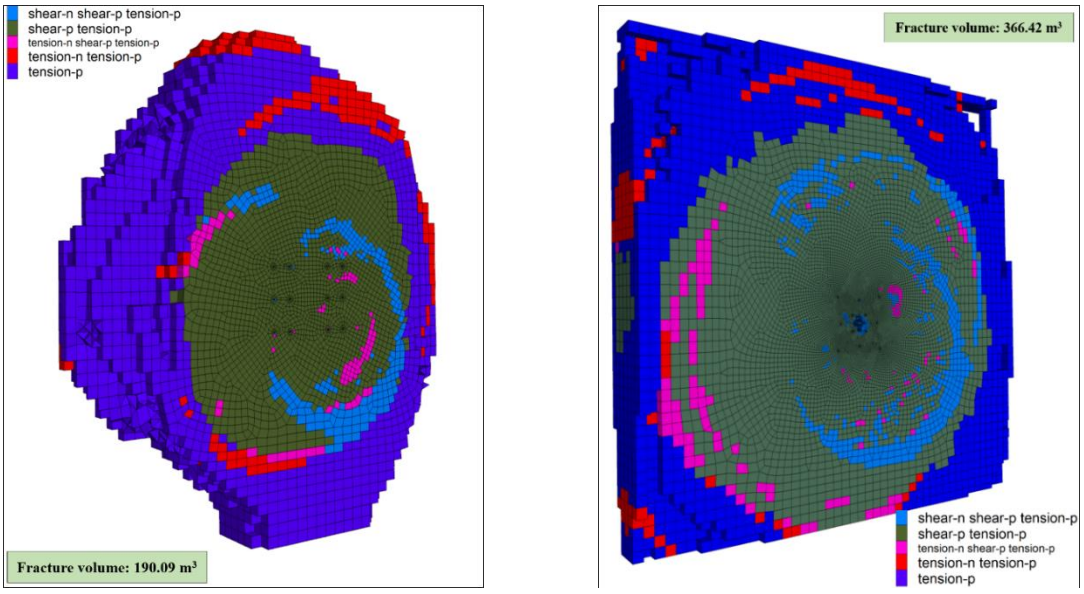

(a) V-cut method (b) Double-drilled parallel cut method

Fig. 15 3D fracture distribution

effective to make the fracture of rock mass and also prevent the amplification of the blasting pressure and vibration.

3.2.3 Fracture area and volume

We analysed the fracture area based on the cross-section of the charge, and obtained values of 110.86 and 184.13 m^2 for the V-cut model and double-drilled parallel cut model, respectively. The value of the double-drilled parallel cut model is larger than that of the V-cut model by 73.27 m^2 (66%) as shown in Table 8.

Fig. 15 shows the 3D fracture distribution extracted from each numerical model. We analysed the fracture volume, using the 3D fracture model, and obtained values of 190.09 and 366.42 m^3 for the V-cut model and double-drilled parallel cut model, respectively. The value of the double-drilled parallel cut model is larger than that of the

Table 8 Fracture area and volume analyzed from numerical analysis

Fracture	V-cut	Double-drilled parallel cut	Difference	Rate of increase compared to V-cut
Area (m^2)	110.86	184.13	73.27	66%
Volume (m^3)	190.09	366.42	176.33	93%

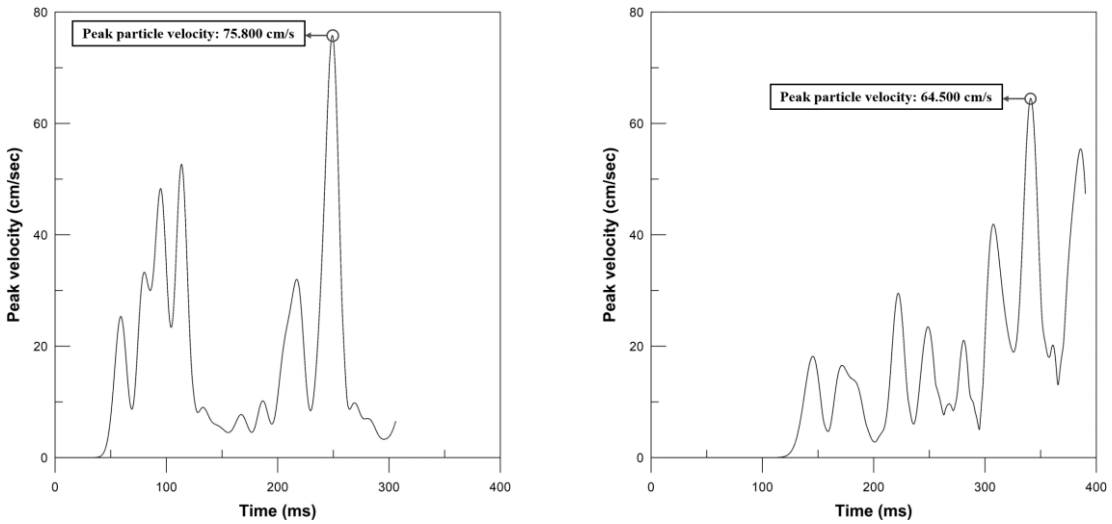

(a) V-cut method (b) Double-drilled parallel cut method

Fig. 16 PPV determined by the models of the V-cut method and the double-drilled parallel method

Table 9 Comparison of the PPVs obtained from field measurement and numerical simulation

Method	Field measurement				Numerical analysis			
	Measurement	Distance (m)	PPV (cm/sec)	Reduction ratio compared to V-cut (%)	Measurement	Distance (m)	PPV (cm/sec)	Reduction ratio compared to V-cut (%)
V-cut	A	59.10	0.097	-	1	8.43	75.800	-
	B	77.89	0.080	-	2	8.43	74.700	-
Double-drilled parallel cut	A	58.58	0.082	15.46	1	8.43	64.500	14.91
	B	77.32	0.043	46.25	2	8.43	60.200	19.41
	Average			30.86	Average			17.16

V-cut model by 176.33 m^2 (93%) as shown in Table 8. Therefore, the double-drilled parallel cut model can fracture rocks more effectively than the V-cut model.

3.2.4 Vibration

Fig. 16 shows the blasting vibration waveform for each model at measurement 1. The PPVs measured in the V-cut method and the double-drilled parallel method are 75.8 and 64.5 cm/sec, respectively, which shows that the PPV measured in the V-cut model is 11.3 cm/sec larger than that in the double-drilled parallel cut model.

According to the numerical analysis, the rock fracture for a part of central cut in the double-drilled parallel cut method is more effective than that in the V-cut method. Likewise, the rock fracture in a double-drilled parallel cut method is more likely to form a free face toward the extended part, thus making lower the blasting vibration in the extended part in the double-drilled parallel cut method than that in the V-cut method.

4. Discussion

This study conducted a comparative analysis of rock fragmentation efficiency and ground vibration controllability between the V-cut method and the double-drilled parallel method, for in-situ test blasting and numerical analysis.

Table 9 compares the PPV values measured in the field and the values obtained from numerical simulations. The limitation of this study is that the vibration measurements were not relatively compared because the numerical model was not made in the field scale. Therefore, the results of the field measurement and the numerical simulations were compared in terms of the reduction ratios of vibration of the two methods in this study.

The PPV measured for the double-drilled parallel cut method was lower than that for the V-cut method in both the field measurements and numerical simulations, with differences of approximately 17% for the numerical analysis and 30% for the field measurements. These differences are acceptable as the numerical simulation does not consider some conditions in the in-situ such as the rock joint conditions. Therefore, blasting simulation with numerical analysis is a suitable indirect method.

According to the field measurements and numerical simulations, the double-drilled parallel cut method could reduce the ground vibration propagation in the tunnel excavation site better than the V-cut method. Furthermore, this numerical technique can be applied to other blasting methods and replace the complicated field operation of blasting excavations.

5. Conclusions

We conducted test blasting operations at a tunnel excavation site to evaluate the effect of reducing blast

vibration in tunneling by the V-cut method and double-drilled parallel cut method. FLAC3D numerical simulation was also carried out to analyze the characteristics of rock fracture propagation and ground vibration controllability, through the V-cut method and double-drilled parallel method. The conclusions of this paper are the following:

- In the field, the PPVs for the whole tunnel blasting part via the double drilled-cut method were 15.46% and 46.25% lower than those via the V-cut method at distances of 59.1 and 77.9 m from the tunnel excavation section, respectively.
- In the numerical simulation, the PPVs for the double drilled-cut method were 17.16% lower than those for the V-cut method.
- The PPV measured in the field was 13.70% lower than that in the numerical analysis. This difference is acceptable as the numerical simulation does not fully consider the in-situ rock mass conditions, such as the rock joint conditions.
- In the numerical simulation, tension and shear fractures occurred more extensively and gradually in the double-drilled parallel cut model than in the V-cut model. Furthermore, the fracture volume for the double drilled-cut method was 176.33 m^3 higher than that for the V-cut method; thus, the double drilled-cut method can fragment rocks more effectively.

To understand the reduction effect of each cut method, maximum possible blasting vibration measurement data should be obtained from field tests. However, there exist various restrictions in obtaining such data, mainly the field conditions and costs. We attempted to overcome this by conducting numerical simulation using FLAC3D.

Though FLAC3D cannot practically explain rock behavior by blasting, it is understood that FLAC3D is highly useful for analyzing fracture propagation aspects and vibration propagation effects.

Furthermore, this numerical technique can be applied to other blasting methods and replace the complicated field operation of blasting excavations.

Acknowledgments

This research was partly supported by Energy & Mineral Resources Development Association of Korea (EMRD) grant funded by the Korea government (MOTIE) (Educational-Industrial Cooperation Consortium of Energy and Mineral Resources Development-Training Program for Specialists in Smart Mining) and National Research Foundation of Korea (NRF) grant funded by the Korea government (MSIT, ME, MOTIE) (NRF-2017M3D8A2085342, the National Strategic Project, Carbon Upcycling).

References

Dimitraki, L.S., Christaras, B.G. and Arampelos, N.D. (2021), "Investigation of blasting impact on limestone of varying quality using FEA", *Geomech. Eng.*, **25**(2), 111-121. https://doi.org/10.12989/gae.2021.25.2.111.

KEI (Korea Environment Institute) (2015), Environmental Impact Statements and Manuals, KEI, Sejong, Korea.

KIGAM (Korea Institute of Geoscience and Mineral Resources) (2021), Big Data Open Platform, KIGAM, Daejeon, Korea.

Kim, N.S. (2016), "Test blasting report for Donghae railway (Pohang-Samcheok)", 11th Section Roadbed, NSB Now ENC, Seoul, Korea.

Lee, M.S. and Kim, H.D. (2016), "Electronic blasting for excavating single line railway tunnel close to residential area", *Explos. Blast.*, **34**(3), 17-20.

Lee, M.S., Kim, H.D., Lee, H. and Lee, J.W. (2018), "Tunnel blasting case by combination of electronic detonator and non-electric detonator", *Explos. Blast.*, **36**(1), 1-9.

Lu, W., Yang, J., Chen, M. and Zhou, C. (2011), "An equivalent method for blasting vibration simulation", *Simul. Model. Pract. Theory*, **19**(9), 2050-2062. https://doi.org/10.1016/j.simpat.2011.05. 012.

National Highway Institute (1991), Rock Blasting and Overbreak Control, Federal Highway Administration, Washington D.C., USA.

Oh, S.Y., Lee, C.S., Lee, K.K., Lee, D.H., Lee, S.J. and Park, J.H. (2017), "A study on the tunnel blasting technique with a combined application of electronic detonators and low vibration explosives in a close proximity to safety things". *Explos. Blast.*, **35**(4), 36-47.

Ozacar, V. (2018), "New methodology to prevent blasting damages for shallow tunnel", *Geomech. Eng.*, **15**(6), 1227-1236. https://doi.org/10.12989/gae.2018.15.6.1227.

Park, D., Jeon, B. and Jeon, S. (2009), "A numerical study on the screening of blast-induced waves for reducing ground vibration", *Rock Mech. Rock Eng.*, **42**(3), 449-473. https://doi.org/10.1007%2Fs00603-008-0016-y.

Qiu, X., Hao, Y., Shi, X., Zhang, S. and Gou, Y. (2018), "Numerical simulation of stress wave interaction in short-delay blasting with a single free surface", *PLOS one*, **13**(9), 1-19. https://doi.org/10.1371/journal.pone.0204166.

Song, Z.P., Li, S.H., Wang, J.B., Liu, J. and Chang, Y.Z. (2017), "Determination of equivalent blasting load considering millisecond delay effect", *Geomech. Eng.*, **15**(2), 745-754. https://doi.org/10.12989/gae.2018.15.2.745.

Starfield, A.M. and Pugliese, J.M. (1968), "Compression waves generated in rock by cylindrical explosive charges: A comparison between a computer model and field measurements", *Int. J. Rock Mech. Min. Sci. Geomech. Abstr.*, **5**(1), 65-77. https://doi.org/10.1016/0148-9062(68)90023-5.

Uyar, G.G. and Aksoy, C.O. (2019), "Comparative review and interpretation of the conventional and new methods in blast vibration analyses", *Geomech. Eng.*, **18**(5), 545-554. https://doi.org/10.12989/gae.2019.18.5.545.

Won, Y.H. and Lee, H. (2007), "Introduction of tunnel blasting method by double-drilled parallel Cut", *Proceedings of the KSEE Conference*, Seoul, Korea, 77-85.

Yilmaz, O. and Unlu, T. (2013), "Three-dimensional numerical rock damage analysis under blasting load", *Tunnel. Undergr. Space Technol.*, **38**, 266-278. https://doi.org/10.1016/j.tust.2013.07.007.

GC